



HAL
open science

An energy residual method for detection of the causes of vibration hypersensitivity

Morvan Ouisse, Jean-Louis Guyader

► **To cite this version:**

Morvan Ouisse, Jean-Louis Guyader. An energy residual method for detection of the causes of vibration hypersensitivity. *Journal of Sound and Vibration*, 2003, 260 (1), pp.83-100. 10.1016/S0022-460X(02)00901-X . hal-00131978

HAL Id: hal-00131978

<https://hal.science/hal-00131978>

Submitted on 13 Mar 2018

HAL is a multi-disciplinary open access archive for the deposit and dissemination of scientific research documents, whether they are published or not. The documents may come from teaching and research institutions in France or abroad, or from public or private research centers.

L'archive ouverte pluridisciplinaire **HAL**, est destinée au dépôt et à la diffusion de documents scientifiques de niveau recherche, publiés ou non, émanant des établissements d'enseignement et de recherche français ou étrangers, des laboratoires publics ou privés.

This document is the author's final manuscript of

M. Ouisse, J. L. Guyader, An energy residual method for detection of the causes of vibration hypersensitivity. *Journal of Sound and Vibration*, 260(1):83 – 100, 2003.

This paper has been published by Elsevier and can be found at
[http://dx.doi.org/10.1016/S0022-460X\(02\)00901-X](http://dx.doi.org/10.1016/S0022-460X(02)00901-X)

AN ENERGY RESIDUAL METHOD FOR
DETECTION OF THE CAUSES OF
VIBRATION HYPERSENSITIVITY

M. OUISSE AND J.L. GUYADER

Address:

Institut National des Sciences Appliquées de Lyon

Laboratoire Vibrations Acoustique

69621 Villeurbanne Cedex, France

Short running headline: DETECTION OF THE CAUSES OF VIBRATION
HYPERSENSITIVITY

Number of pages: 36

Summary:

This work deals with hypersensitive vibration behavior of plates. The aim of the proposed method is to detect structural zones inducing such behavior. It is based on a residual calculation, which takes into account structural uncertainties, and has a low numerical cost since it requires only the resolution of the problem for the nominal structure. Then, this solution is used to calculate energy residuals on different parts of perturbed structures in order to detect which zones will produce an hypersensitive behavior. Basis of the method are first developed on a simple problem, a rod, and then applied on a typical hypersensitive structure, a plates network. Finally one can show that the proposed tool is able to detect which zones of the plates network are responsible for hypersensitive behavior.

1 Introduction

Because of manufacturing cost, uncertainties in structural parameters are inevitable, bringing dispersions in eigenfrequencies and responses of the structures, which can induce acoustical problems when shifted structural eigenfrequencies are coinciding with cavity ones. In this way, two objects manufactured with the same constraints can have very different acoustical behavior. Fortunately, in most of cases, this problem does not exist, and uncertainties in manufacturing processes are expected to entail small variations in eigen values, eigen vectors and responses of structures, allowing one to predict the behavior of a set of structures on the basis of results obtained for the nominal one. Hypersensitivity appears when these dispersions become larger, bringing large differences between the nominal structure and some of other structures belonging to the same manufacturing set. This problem has been raised many times, and many people are interested in reducing dispersion without increasing manufacturing cost. In references [1] and [2], measurements results are shown on nominally identical structures, and many differences can be observed on the whole frequency domain, although these papers are mainly related on effects of uncertainties in high frequency range. Results presented by Bernhard [2] concern frequency responses for sound pressure due to mechanical excitation for a population of 98 nominally identical vehicles. Large differences can be observed, almost in medium and high frequency range. Frequency responses of vibrating 3-beams systems are used to understand these behaviors. Similar results have been presented by Fahy [1], concerning 41 nominally identical structures.

Many existing methods allow one to evaluate dispersion but only when uncertainties are small: statistical dynamics is a classical field of research ([3], [4], [5]).

But if a given parameter is hypersensitive, in other words if a small variation of this parameter brings a large variation of the response, those methods are unable to evaluate the corresponding dispersion. Nevertheless, several ways can be efficient to estimate response sensitivity for small variations of parameters: many stochastic approaches have been developed, some of them need a low calculation time (FORM, SORM), given good results for small variations or particular cases, while other ones are more expensive but have a better accuracy or are developed to be integrated with existing methods, like FEM [6]. Among new developments, fuzzy methods may be mentioned [7], [8], but likewise stochastic methods, when the formulation is adapted for large variations of input parameters, a good agreement with real dispersion values can be obtained only if the calculation time is about the same as in a Monte Carlo simulation, which is still the only method capable to estimate correctly response sensitivity in any cases, even if hybrid methods using partial Monte Carlo simulations are thinkable [9].

An alternative way to these high calculation cost methods for hypersensitivity cases could be to develop a tool that would be able to detect, without high calculation time, from which part of the structure are issued causes of high sensitivity. This tool could be used to direct a design modification of sensitive parts in order to reduce response dispersions. Following this concept, we have developed a method that is based on the only resolution of the nominal problem, used for estimation of an a posteriori error, which supplies an indicator evaluated on the whole structure, or on different parts of it, and then allows one to detect causes of hypersensitivity. In this paper we present a theoretical background, necessary before explanation of our method, which is developed in detail on a typical hypersensitive structure.

2 Theoretical background

The aim of this part is to present a short description of the tool used here. A simple way to understand the basic ideas of the tool is to consider a simple problem, like a displacement description of a forced longitudinal vibrating structure (figure 1). The classical local formulation of the problem can be written in the following terms: The displacement field U must verify the equation of motion:

$$\frac{d}{dx} \left[ES_1 \frac{dU}{dx} \right] + \omega^2 \rho S_1 U = 0 \text{ in } I_1 =]0, x_0[\quad (1)$$

$$\frac{d}{dx} \left[ES_2 \frac{dU}{dx} \right] + \omega^2 \rho S_2 U = F \text{ in } I_2 =]x_0, L[\quad (2)$$

According to the boundary conditions:

$$U|_{x=0} = U_0 \quad (3)$$

$$ES_2 \frac{dU}{dx} |_{x=L} = F_0 \quad (4)$$

while continuity of forces and displacements for $x = x_0$ imposes:

$$U|_{x=x_0^-} = U|_{x=x_0^+} \quad (5)$$

$$ES_1 \frac{dU}{dx} |_{x=x_0^-} = ES_2 \frac{dU}{dx} |_{x=x_0^+} \quad (6)$$

where U_0 is known and the notation $U|_{x=x_0^-}$ indicates the value of U extended by continuity on $x = x_0$ with $x \leq x_0$.

Usually, everything in the previous equations is known except the displace-

ment field U . The solution U_{sol} of this problem can be calculated with different methods. One way to obtain it, is to find the field that minimizes the residual 7:

$$\begin{aligned}
R(U) = & \frac{ES_1}{L} \left(U_{|x=0} - U_0 \right)^2 + \frac{1}{2} \int_{I_1} \frac{1}{\omega^2 \rho S_1} \left(\frac{d}{dx} \left[ES_1 \frac{dU}{dx} \right] + \omega^2 \rho S_1 U \right)^2 dx + \\
& + \frac{ES_1}{L} \left(U_{|x=x_0^-} - U_{|x=x_0^+} \right)^2 + \frac{L}{ES_1} \left(ES_1 \frac{dU}{dx} \Big|_{x=x_0^-} - ES_2 \frac{dU}{dx} \Big|_{x=x_0^+} \right)^2 \quad (7) \\
& + \frac{1}{2} \int_{I_2} \frac{1}{\omega^2 \rho S_2} \left(\frac{d}{dx} \left[ES_2 \frac{dU}{dx} \right] + \omega^2 \rho S_2 U - F \right)^2 dx + \frac{L}{ES_2} \left(ES_2 \frac{dU}{dx} \Big|_{x=L} - F_0 \right)^2
\end{aligned}$$

This residual has interesting properties:

$R(U)$ is stationary if and only if $U = U_{sol}$, which means that the solution can be found using numerical approaches;

$R(U) \geq 0$ and $R(U_{sol}) = 0$, which means that the steadiness of the residual is a minimum and that the residual can be used to estimate the quality of a solution. If an approximate solution field U_{app} has been calculated on the domain $\Omega = [0, L]$, the value of $R(U_{app})$ is a measurement of the difference between U_{sol} and U_{app} .

This residual has been derived using natural weighting of the various terms, in order that it could be linked to energy and work expressions, although these weights values are not mathematically necessary to keep the above properties true.

Moreover, a localization of differences between the two fields can be performed using a decomposition of the residual along the rod: $R(U) = R_1(U) + R_2(U) + R_3(U) + R_4(U) + R_5(U)$, where:

$$\begin{aligned}
R_1(U) &= \frac{ES_1}{L} \left(U|_{x=0} - U_0 \right)^2 \\
R_2(U) &= \frac{1}{2} \int_{I_1} \frac{1}{\omega^2 \rho S_1} \left(\frac{d}{dx} \left[ES_1 \frac{dU}{dx} \right] + \omega^2 \rho S_1 U \right)^2 dx \\
R_3(U) &= \frac{ES_1}{L} \left(U|_{x=x_0^-} - U|_{x=x_0^+} \right)^2 + \frac{L}{ES_1} \left(ES_1 \frac{dU}{dx} |_{x=x_0^-} - ES_2 \frac{dU}{dx} |_{x=x_0^+} \right)^2 \quad (8) \\
R_4(U) &= \frac{1}{2} \int_{I_2} \frac{1}{\omega^2 \rho S_2} \left(\frac{d}{dx} \left[ES_2 \frac{dU}{dx} \right] + \omega^2 \rho S_2 U - F \right)^2 dx \\
R_5(U) &= \frac{L}{ES_2} \left(ES_2 \frac{dU}{dx} |_{x=L} + F_0 \right)^2
\end{aligned}$$

If the field U used for the estimation is not U_{sol} , at least one of the values of $R_i(U)$ is different from zero, allowing one to know on which part of the structure the field is not correct. Let's note that R_2 and R_4 can be decomposed in many parts in order to have a better localization of errors.

These expressions are very similar to those which are used for adaptive mesh in vibration analysis, fundamental works have been presented by Ladevèze [10] and Babuska [11], while Verfurth gives in [12] an overview of the most popular error estimators. As far as acoustic field is concerned, Bouillard has adapted these methods in [13].

Another application of error in the constitutive law has been presented by Guyader in [14], relating to bounding of eigenfrequencies of imperfectly characterized structures. This work shows the validity of Love-Kirchhoff plate assumption, but as far as bounding is concerned, calculated eigenfrequencies boundaries are unfortunately often very large.

3 A method for hypersensitivity causes detection

Many methods are able to determine the sensitivity of a result according to a given parameter, but none of them allows one to detect structural causes of

hypersensitivity. This is the aim of this paper. Until now, the only efficient way to detect these causes is to perform a high cost Monte-Carlo simulation, solving many times the problem. We propose here an alternative way of low numerical cost:

First, the problem must be solved with nominal parameters. That is to find the displacement field U_{sol} verifying equations 1 to 6. Let us say that if the displacement field is a good approximation of the exact solution, then using it in the residual should give a result close to zero.

Then, using residual 8 adapted to the structure, its variable parameters and solution of the nominal problem allows one to estimate the quality of the solution field of the nominal problem in perturbed operators. For each chosen part of the structure on which we perform this post processing calculation, the estimator indicates the sensitivity according to variable parameters.

This method requires only one resolution of the whole problem, then the nominal solution field is used to perform the calculation of an estimator on perturbed structures.

4 A structure with a high sensitivity

To demonstrate the interest of the proposed method, one requires highly sensitive structures. A relatively simple analytic one is a network of plates. Rebillard and Guyader have shown [15] that the sensitivity of two plates (figure 8) coupled with an angle θ was maximum for a nominal value of the connecting angle θ of 4° , so the structure presented on figure 2 presents three presumed hypersensitive connections, which are numbered 4, 5 and 7. If connecting angle θ does not exist, there is not reflected wave, the entire incident one is fully transmitted. As soon as

θ has a non-null value, transmitted power decreases quickly, and coupling effects between in-plane and bending movements imply that the most sensitive angle has a value of 4 degrees. This value depends on chosen geometry and structural parameters [16]. The analytical model used is presented in [15] and consists in a semi-modal decomposition combined to a wave formulation, and takes into account coupling effects between flexural and in-plane motions due to connecting angles.

The steel plates ($E = 2.10^{11} Pa$, $\eta = 10^{-2}$, $\nu = 0,3$) have a common width of 40 cm and thickness of 2 mm. The structure, which could be a kind of hood of a machine is contained in a box of size 0,4m x 0,54m x 1,7m. The plates are simply supported on the uncoupled sides, and the connecting angles can be classified in two categories: hypersensitive for numbers 4, 5 and 7 (their nominal value is 4°), while the other ones are not sensitive (45° , 86° and 90° for nominal values).

In order to study sensitivity of angular parameters, let's assume that their values are randomly distributed in a 1° range around the nominal one. A Monte-Carlo simulation allows one to confirm the high sensitivity of connecting angles. Figure 3 shows variability of flexural velocity response on plate located between angles 7 and 8, when an harmonic excitation is applied on plate located between angles 1 and 2. Connecting angles 1 to 8 are chosen in a random way, according to their nominal value with a 1° uncertainty (Gaussian distribution, with a $1/6$ degree standart deviation).

The sensitivity is important, almost in the band 140-200 Hz. We can determine the influence of each connecting angle on the frequency range 150-200 Hz: figure 4 shows the variability of the response when only angle 4 is varying, figure 5 for angle 5, figure 6 for angle 7. Then, figure 7 allows one to conclude that other connecting angles have a very small sensitivity. These remarks are made

without using any measure for hypersensitivity, which could be done in many ways. Such a tool could be based among other things on differences of eigenvalues, or modulus of response at a precise frequency or on a range [15], and one could take into account one or many statistical moments of variables, but this is not the purpose of this work. What matters here is that the considered structure is highly sensitive to identified parameters, and this can be done easily observing figures 4 to 6.

In conclusion, the developed method should be able to detect, with the residual, the three angles numbered 4, 5 and 7 as hypersensitive ones.

5 Application of the method on hypersensitive structure

5.1 One simple example : a rod of variable cross section

What we are expecting when applying the method is detection of connecting angles 4, 5 and 7 as hypersensitive ones. In order to apply the proposed method on the previously presented case, we need an expression of the residual adapted to plates. However, because the mathematical expression to handle for plates are complicated, we first present the simple case of a rod of variable cross section at point x_0 , like the one presented on figure 1. The equations that have to be verified in this case are numbered 1 to 6. The solution U_{sol} of this problem is expected to be known, and of course verifies equations 1 to 6. Moreover, using this displacement field in residual 7 or 8 brings to a null value. Let's consider another structure, which is the same as the previous one, except its section size $S'_1 \neq S_1$ on part $I_1 =]0, x_0[$ of the rod. If we consider structural operators of this

second rod, using the solution U_{sol} of the first problem brings to:

$$\frac{d}{dx} \left[ES'_1 \frac{dU_{sol}}{dx} \right] + \omega^2 \rho S'_1 U_{sol} = 0 \text{ in } I_1 =]0, x_0[\quad (9)$$

$$\frac{d}{dx} \left[ES_2 \frac{dU_{sol}}{dx} \right] + \omega^2 \rho S_2 U_{sol} = F \text{ in } I_2 =]x_0, L[\quad (10)$$

$$U_{sol}|_{x=0} = U_0 \quad (11)$$

$$ES_2 \frac{dU_{sol}}{dx} \Big|_{x=L} = F_0 \quad (12)$$

$$U_{sol}|_{x=x_0^-} = U_{sol}|_{x=x_0^+} \quad (13)$$

$$ES'_1 \frac{dU_{sol}}{dx} \Big|_{x=x_0^-} \neq ES_2 \frac{dU_{sol}}{dx} \Big|_{x=x_0^+} \quad (14)$$

The only equation that U_{sol} does not verify is the one relative to continuity of normal force in x_0 (eq. 14). Using residual expression 8 adapted to the second structure (using S'_1 instead of S_1) with solution U_{sol} one obtain:

$$\begin{aligned} R'_1(U_{sol}) &= \frac{ES'_1}{L} (U_{sol}|_{x=0} - U_0)^2 = 0 \\ R'_2(U_{sol}) &= \frac{1}{2} \int_{I_1} \frac{1}{\omega^2 \rho S'_1} \left(\frac{d}{dx} \left[ES'_1 \frac{dU_{sol}}{dx} \right] + \omega^2 \rho S'_1 U_{sol} \right)^2 dx = 0 \\ R'_3(U_{sol}) &= \frac{ES'_1}{L} (U_{sol}|_{x=x_0^-} - U_{sol}|_{x=x_0^+})^2 + \frac{L}{ES_1} \left(ES'_1 \frac{dU_{sol}}{dx} \Big|_{x=x_0^-} - ES_2 \frac{dU_{sol}}{dx} \Big|_{x=x_0^+} \right)^2 \neq 0 \\ R'_4(U_{sol}) &= \frac{1}{2} \int_{I_2} \frac{1}{\omega^2 \rho S_2} \left(\frac{d}{dx} \left[ES_2 \frac{dU_{sol}}{dx} \right] + \omega^2 \rho S_2 U_{sol} - F \right)^2 dx = 0 \\ R'_5(U_{sol}) &= \frac{L}{ES_2} \left(ES_2 \frac{dU_{sol}}{dx} \Big|_{x=L} + F_0 \right)^2 = 0 \end{aligned} \quad (15)$$

The only part of the residual which is not zero is the third part $R'_3(U)$. It is related to equations 13 (which is verified, so the first term of R'_3 does vanish) and 14 (which is not verified):

$$R'_3(U_{sol}) = \frac{L}{ES_1} \left(ES'_1 \frac{dU_{sol}}{dx} \Big|_{x=x_0^-} - ES_2 \frac{dU_{sol}}{dx} \Big|_{x=x_0^+} \right)^2 \neq 0$$

Of course this expression has been derived from 1-D formulation, and needs to be adapted to our plates network problem. But before this derivation, let's remark that the estimator corresponding to R_3 that we will use will be a relative one, in order to have a non dimensional quantity:

$$e_3(U) = \frac{\frac{ES}{L} (U|_{x=x_0^-} - U|_{x=x_0^+})^2 + \frac{L}{ES} \left(ES \frac{dU}{dx} \Big|_{x=x_0^-} - ES \frac{dU}{dx} \Big|_{x=x_0^+} \right)^2}{\frac{ES}{L} (U|_{x=x_0^-} + U|_{x=x_0^+})^2 + \frac{L}{ES} \left(ES \frac{dU}{dx} \Big|_{x=x_0^-} + ES \frac{dU}{dx} \Big|_{x=x_0^+} \right)^2} \quad (16)$$

5.2 The plates network

The detailed adapted formulation for our problem is given here, according to notations defined on figure 8. In this part we are interested only by sensitivity due to connecting angles. All other parameters are supposed to keep their nominal values. This means that the nominal solution satisfies all the equations of the problem with varied angles except continuity conditions at plates junctions. According to that, we will not develop the expression of the whole residual corresponding to equation 8, but only the one corresponding to equation 16, adapted to the plates network formulation, which is given here. Let us define:

the displacement field on plate i : $\vec{U}_i = u_i(x_i, y) \vec{x}_i + v_i(x_i, y) \vec{y} + w_i(x_i, y) \vec{z}_i$

the flexural rotation on plate i along axis \vec{y} : $\vec{R}_i \cdot \vec{y} = R_i(x_i, y)$

the generalized forces on plate i : $\vec{F}_i = F_{x,i}(x_i, y)\vec{x}_i + F_{y,i}(x_i, y)\vec{y} + F_{z,i}(x_i, y)\vec{z}_i$
and the generalized momentum on plate i along axis \vec{y} : $\vec{M}_i \cdot \vec{y} = M_i(x, y)$

These quantities are linked by continuity conditions 17 to 24, that assume rigid connections at plates junctions: $\forall y \in [0, a]$

$$u_{i+1}(0, y) = u_i(l_i, y) \cos \theta_{i+1} + w_i(l_i, y) \sin \theta_{i+1} = u_i^*(l_i, y) \quad (17)$$

$$v_{i+1}(0, y) = v_i(l_i, y) \quad (18)$$

$$w_{i+1}(0, y) = w_i(l_i, y) \cos \theta_{i+1} - u_i(l_i, y) \sin \theta_{i+1} = w_i^*(l_i, y) \quad (19)$$

$$F_{x,i+1}(0, y) = F_{x,i}(l_i, y) \cos \theta_{i+1} + F_{z,i}(l_i, y) \sin \theta_{i+1} = F_{x,i}^*(l_i, y) \quad (20)$$

$$F_{y,i+1}(0, y) = F_{y,i}(l_i, y) \quad (21)$$

$$F_{z,i+1}(0, y) = F_{z,i}(l_i, y) \cos \theta_{i+1} - F_{x,i}(l_i, y) \sin \theta_{i+1} = F_{z,i}^*(l_i, y) \quad (22)$$

$$R_{i+1}(0, y) = R_i(l_i, y) \quad (23)$$

$$M_{i+1}(0, y) = M_i(l_i, y) \quad (24)$$

Note that the star symbol (e.g. in $u_i^*(l_i, y)$) is used here in order to simplify notations, and that all equations must be satisfied $\forall y \in [0, a]$. Then we can define the estimator 25, based on expression 16 :

$$e = \frac{\int_{\partial\Omega} \frac{Eh}{a(1-\nu^2)} (u_{i+1} - u_i^*)^2 d\Omega + \int_{\partial\Omega} \frac{Eh}{2a(1+\nu)} (v_{i+1} - v_i^*)^2 d\Omega + \int_{\partial\Omega} \frac{D}{a^3} (w_{i+1} - w_i^*)^2 d\Omega + \dots}{\int_{\partial\Omega} \frac{Eh}{a(1-\nu^2)} (u_{i+1} + u_i^*)^2 d\Omega + \int_{\partial\Omega} \frac{Eh}{2a(1+\nu)} (v_{i+1} + v_i^*)^2 d\Omega + \int_{\partial\Omega} \frac{D}{a^3} (w_{i+1} + w_i^*)^2 d\Omega + \dots} \quad (25)$$

$$\frac{\dots + \int_{\partial\Omega} \frac{a(1-\nu^2)}{Eh} (F_{x,i+1} - F_{x,i}^*)^2 d\Omega + \int_{\partial\Omega} \frac{2a(1+\nu)}{Eh} (F_{y,i+1} - F_{y,i}^*)^2 d\Omega + \dots}{\dots + \int_{\partial\Omega} \frac{a(1-\nu^2)}{Eh} (F_{x,i+1} + F_{x,i}^*)^2 d\Omega + \int_{\partial\Omega} \frac{2a(1+\nu)}{Eh} (F_{y,i+1} + F_{y,i}^*)^2 d\Omega + \dots}$$

$$\begin{aligned} & \dots + \int_{\partial\Omega} \frac{a^3}{D} (F_{z,i+1} - F_{z,i}^*)^2 d\Omega + \int_{\partial\Omega} \frac{D}{a} (R_{i+1} - R_i^*)^2 d\Omega + \int_{\partial\Omega} \frac{a}{D} (M_{i+1} - M_i^*)^2 d\Omega \\ & \dots + \int_{\partial\Omega} \frac{a^3}{D} (F_{z,i+1} + F_{z,i}^*)^2 d\Omega + \int_{\partial\Omega} \frac{D}{a} (R_{i+1} + R_i^*)^2 d\Omega + \int_{\partial\Omega} \frac{a}{D} (M_{i+1} + M_i^*)^2 d\Omega \end{aligned}$$

Where integration domains $\partial\Omega$ are coupling lines and a is the common width of the plates. With such an expression, the method can now be applied on the plates network.

The first step is the resolution of the nominal system, using the semi-modal decomposition. For a given frequency, the calculation provides the solution field on the structure. See [15] for details.

To perform the second step, variables parameters must be defined. In the present case, these are connecting angles. So each angle is supposed to have a Gaussian distribution, on a 1 degree width range (1/6 degree standard deviation). Locations chosen for the evaluation of estimator are the coupling lines, for each of these the calculation of expression 25 is carried out, using the displacement field solution of the nominal problem. These calculations are performed using angles randomly chosen in the range, and at last the mean of 40 evaluations for each coupling line is presented, for both frequencies 175 and 195 Hz.

Figure 9 clearly shows that the estimator is able to detect connecting angles which bring hypersensitive behavior. Using nominal solution field in perturbed estimator bring to a near zero result for other angles, where as those with a nominal value of 4 degrees lead to a big residual.

6 Hypersensitivity fast detection

The first aim of the method is a fast detection of hypersensitive zones, so the number of cases used for evaluation of the mean of estimators should be small, since calculation time grows up with the number of cases. The method is then ap-

plied with only three evaluations of estimators. Figure 10 clearly shows that two consecutive calculations do not give the same results, which is obvious considering the high sensitivity of parameters. Nevertheless, each of the three hypersensitive zones can be detected, allowing one to obtain a very fast detection of these areas.

7 Hypersensitivity causes versus frequency

The presented method allows one to determine sensitivities causes for several frequencies. The calculation performed on a frequency range are presented on figure 11, which shows the influence of connecting angles versus frequency, on the 80-200 Hz band. The agreement with figures 4 to 6 is good, since each time the estimator indicates a low value, the sensitivity of the parameter is weak. This can be observed for angle 4 at 115 Hz or for angle 5 at 142 Hz. Large values of residual indicates that the connecting angle is highly sensitive, but the value itself has not been related to any sensitivity value of the response. As far as connecting angle 7 is concerned, residual indicates that its sensitivity goes down between 150 and 200Hz, and this is in agreement with fig.6. On the other hand, for particular frequencies like 125 Hz (for angle 7), the Monte Carlo analysis seems to show that the sensitivity is weak, whereas the estimator is not able to detect it. The reason for this difference is that the proposed estimators are global ones, and take into account the solution field on whole structure, even if the post processing calculation are performed only on a part of it, whereas sensitivity figures 4 to 6 are obtained with a calculation on a particular point of the structure. This means that if we perform another Monte Carlo calculation with the same excitation as the one used for figure 6, but measuring displacement response on another point on the same plate, the parameter will be more sensitive, as shown on figure 12.

This phenomenon can be easily understood if the point used for the evaluation of estimator is located on a node.

8 First order analysis of estimators

As far as our particular structure is concerned, it is possible to obtain an analytical expression of the mean of estimators, using a first order decomposition relating to varying angle. Let's suppose that the connecting angle $\theta = \bar{\theta} + \theta'$ has a nominal value $\bar{\theta}$ and that its variation is $|\bar{\theta} - \theta'| \ll 1$. The first order estimation of equation 25 is developed here. The fields which are not signed with a star are supposed to verify equations 17 to 24, according to angle $\bar{\theta}$ while those with a star do not exactly verify them, because of $\bar{\theta}$.

The first step is to evaluate the first term of equation 25 using equation 17.

$$(u_{i+1}(0, y) - u_i^*(L_i, y))^2 = (u_{i+1} - u_i \cos\theta - w_i \sin\theta)^2$$

Using the first order decomposition of sinusoidal functions $\cos\theta \simeq \cos\bar{\theta} - \theta' \sin\bar{\theta}$ and $\sin\theta \simeq \sin\bar{\theta} + \theta' \cos\bar{\theta}$ brings to:

$$(u_{i+1} - u_i^*)^2 = \theta'^2 (u_i \sin\bar{\theta} - w_i \cos\bar{\theta})^2$$

As far as the fields relating to y axis are concerned, our assumption is that the nominal calculation is correct, so equations 18, 21, 23, and 24 are verified:

$$v_{i+1} - v_i^* = 0 ; F_{y,i+1} - F_{y,i}^* = 0$$

$$R_{i+1} - R_i^* = 0 ; M_{i+1} - M_i^* = 0$$

A similar calculation can be performed in order to estimate other terms of the numerator in equation 25 and lastly, assuming that 0th-order terms are larger than first order one, the evaluation of estimator is:

$$e = \frac{\int_{\partial\Omega} \theta'^2 \left[\frac{Eh}{a(1-\nu^2)} (u_i \sin\bar{\theta} - w_i \cos\bar{\theta})^2 + \frac{D}{a^3} (u_i \cos\bar{\theta} + w_i \sin\bar{\theta})^2 + \dots \right.}{4 \int_{\partial\Omega} \left[\frac{Eh}{a(1-\nu^2)} u_{i+1}^2 + \frac{Eh}{2a(1+\nu)} v_{i+1}^2 + \frac{D}{a^3} w_{i+1}^2 + \frac{D}{a} R_{i+1}^2 + \dots \right.} \\ \left. \dots + \frac{a(1-\nu^2)}{Eh} (F_{x,i} \sin\bar{\theta} - F_{z,i} \cos\bar{\theta})^2 + \frac{a^3}{D} (F_{x,i} \cos\bar{\theta} + F_{z,i} \sin\bar{\theta})^2 \right] d\Omega} \\ \left. \dots + \frac{a(1-\nu^2)}{Eh} F_{x,i+1}^2 + \frac{2a(1+\nu)}{Eh} F_{y,i+1}^2 + \frac{a^3}{D} F_{z,i+1}^2 + \frac{a}{D} M_{i+1}^2 \right] d\Omega}$$

If we consider only the first order estimation, this estimator is proportional to θ'^2 and a statistical calculation can be performed to determine its mean. Denoting $\sigma_{\theta'}$ the standart deviation of θ' and assuming a Gaussian centered distribution :

$$f_{\theta'}(\mu) = \frac{1}{\sigma_{\theta'} \sqrt{2\pi}} \exp\left(-\frac{\mu^2}{2\sigma_{\theta'}^2}\right)$$

we can calculate the distribution of θ'^2 , which is zero on $]-\infty, 0[$, and on $]0, +\infty[$:

$$f_{\theta'^2}(\mu) = \frac{1}{\sigma_{\theta'} \sqrt{2\pi\mu}} \exp\left(-\frac{\mu}{2\sigma_{\theta'}^2}\right)$$

This can be found using the cumulative distribution function $F_{\theta'^2}(k) = P(\theta'^2 \leq k) = P(-\sqrt{k} \leq \theta' \leq \sqrt{k})$

$$F_{\theta'^2}(k) = \int_{-\sqrt{k}}^{+\sqrt{k}} f_{\theta'}(\mu) d\mu = \int_0^{\sqrt{k}} \frac{2}{\sigma_{\theta'} \sqrt{2\pi}} \exp\left(-\frac{\mu^2}{2\sigma_{\theta'}^2}\right) d\mu$$

using the substitution $t = \mu^2$ brings to:

$$F_{\theta'^2}(k) = \int_0^k \frac{1}{\sigma_{\theta'} \sqrt{2\pi t}} \exp\left(-\frac{t}{2\sigma_{\theta'}^2}\right) dt$$

Then one can evaluate the mean of θ'^2 :

$$E(\theta'^2) = \int_0^\infty \mu f_{\theta'^2}(\mu) d\mu = \sigma_{\theta'}^2 \frac{2}{\sqrt{\pi}} \int_0^\infty \exp(-t^2) dt = \sigma_{\theta'}^2$$

Finally this brings one to estimate the first order mean of the residual:

$$e_{first\ order} = \sigma_{\theta'}^2 \frac{\int_{\partial\Omega} \left[\frac{Eh}{a(1-\nu^2)} (u_i \sin\bar{\theta} - w_i \cos\bar{\theta})^2 + \frac{D}{a^3} (u_i \cos\bar{\theta} + w_i \sin\bar{\theta})^2 + \dots \right.}{4 \int_{\partial\Omega} \left[\frac{Eh}{a(1-\nu^2)} u_{i+1}^2 + \frac{Eh}{2a(1+\nu)} v_{i+1}^2 + \frac{D}{a^3} w_{i+1}^2 + \frac{D}{a} R_{i+1}^2 + \dots \right.} \quad (26)$$

$$\left. \dots + \frac{a(1-\nu^2)}{Eh} (F_{x,i} \sin\bar{\theta} - F_{z,i} \cos\bar{\theta})^2 + \frac{a^3}{D} (F_{x,i} \cos\bar{\theta} + F_{z,i} \sin\bar{\theta})^2 \right] d\Omega}{\left. \dots + \frac{a(1-\nu^2)}{Eh} F_{x,i+1}^2 + \frac{2a(1+\nu)}{Eh} F_{y,i+1}^2 + \frac{a^3}{D} F_{z,i+1}^2 + \frac{a}{D} M_{i+1}^2 \right] d\Omega}$$

This expression allows one to have a very fast obtaining of estimator frequency evolution, since only one post processing calculation has to be performed. Figure 13 shows the frequency evolution of estimator 2, and has to be compared with figure 11. First order estimation is close to Monte Carlo simulation, little differences are due to higher order terms, but the first order estimation is close to the expected result.

Finally, for this particular case, the first order analysis is a very fast way to obtain pertinent informations about frequency evolution of estimator. One should precise that this first order analysis is not necessary to find structural zones which are responsible for hypersensitive behavior, like shown on part 6. Nevertheless, it allows one to obtain more precise results. In our case, there is only one structural parameter which is supposed to vary, and first order analysis expression is quite easy to obtain. For a different structure, with many varying

parameters, there could be a main difference for the first order analysis which is the impossibility to obtain an analytical expression of estimator like equation 26 that should be evaluated numerically, with a calculation cost growing with the number of parameters. However, if we are interested only by first order estimation, computational time will be much less intensive than a Monte Carlo approach.

9 Conclusions

A new tool has been presented for vibration hypersensitivity causes detection. It is based on the concept of post processing error estimation, since only the nominal problem is solved, then the solution is used in a residual functional to localize hypersensitive zones. After a short theoretical background, a specific formulation has been developed and tested on a hypersensitive structure. The proposed method is able to detect hypersensitive zones of the structure, for the studied case three particular connecting angles have been successfully localized. A quick analysis can be performed in order to have a fast estimation of hypersensitive zones, even if results can not be very precise. Another point is that the tool is able to supply a frequency evolution of hypersensitive zones, and for our particular structure a first order analysis has been performed and brings satisfactory results. The next step in the evolution of our method will be an FEM implementation.

References

- [1] F. FAHY 1993 *Proceedings of Inter-Noise 93, Leuven, Belgium*, **1**, 13–26. Statistical energy analysis: A wolf in sheep’s clothing?
- [2] R. BERNHARD 1996 *Proceedings of Inter-Noise 96, Liverpool, England*, 2867–2872. The limits of predictability due to manufacturing and environmentally induced uncertainty.
- [3] P. CARAVANI and W. THOMAS 1973 *AIAA Journal* **11**, no. 2, 170–173. Frequency response of a dynamic system with statistical damping.
- [4] P. CHEN and W. SOROKA 1974 *Journal of Sound and Vibration* **37**, no. 4, 547–556. Multidegree dynamic response of a system with statistical properties.
- [5] R. IBRAHIM 1987, *Applied Mechanics Review* **40**, no. 3, 309–328. Structural dynamics with parameters uncertainties.
- [6] R. GHANEM and P. SPANOS, 1991, New York, Berlin. *Stochastic Finite Elements: A Spectral Approach*.
- [7] S. RAO and J. SAWYER 1995 *AIAA Journal* **33**, no. 12, 2364–2370. Fuzzy finite elements approach for the analysis of imprecise defined systems.
- [8] D. MOENS and D. VANDEPITTE 1999 *Proceedings of Euromech 405: Numerical Modelling Of Uncertainties*, 93–101. A method for the calculation of fuzzy frequency response functions of uncertain structures based on modal superposition.

- [9] E. BLAIN, D. AUBRY, P. CHOVE, and P. LARDEUR 1999 *Proceedings of Euromech 405: Numerical Modelling Of Uncertainties*, 1–6. Influence of parameters dispersion on the vibrating behaviour of spot welded plates.
- [10] P. LADEVEZE and D. LEGUILLON 1983 *SIAM Journal on Numerical Analysis* **20**, 485–509. Error estimate procedure in the finite element method and applications.
- [11] I. BABUSKA 1978 *International Journal for Numerical Methods in Engineering* **12**, 1597–1615. A posteriori error estimates for the finite element method,
- [12] R. VERFURTH 1999 *Computer Methods In Applied Mechanics And Engineering* **176**, 419–440. A review of a posteriori error estimation techniques for elasticity problems.
- [13] P. BOUILLARD and F. IHLENBURG 1999 *Computer Methods In Applied Mechanics And Engineering* **176**, 147–163. Error estimation and adaptivity for the finite element method in acoustics: 2D and 3D applications.
- [14] J.L. GUYADER 1987 *Journal of Theoretical and applied mechanics* **6**, no. 2, 231–252. Free vibrations of imperfectly characterized elastic continuous media. application to the validity of love-kirchhoff plate assumption.
- [15] E. REBILLARD and J.L. GUYADER 1995 *Journal of Sound and Vibration* **188**, no. 3, 435–454. Vibrational behaviour of a population of coupled plates: hypersensitivity to the connexion angle.
- [16] M. OUISSE and J.L. GUYADER 2002, Internal report, *LVA - INSA Lyon*. Sensitivity of coupled 1D and 2D systems responses: a wave approach.

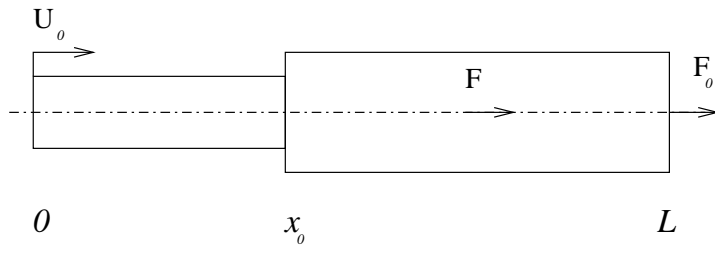


Figure 1: Rod model

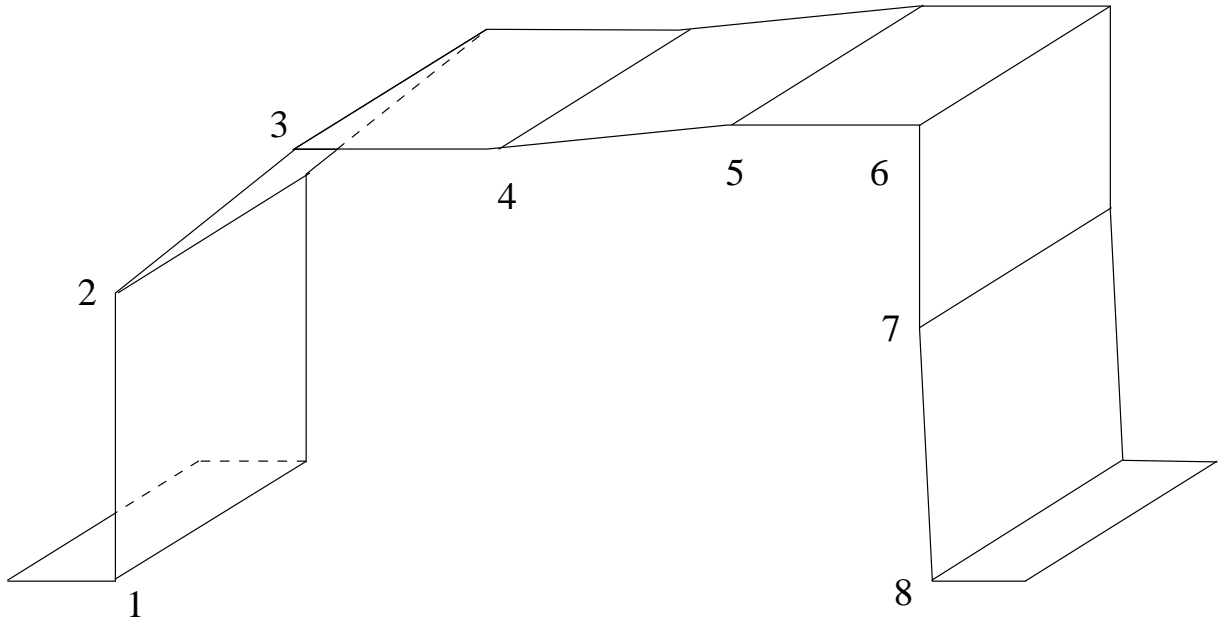


Figure 2: Steel plates hypersensitive structure

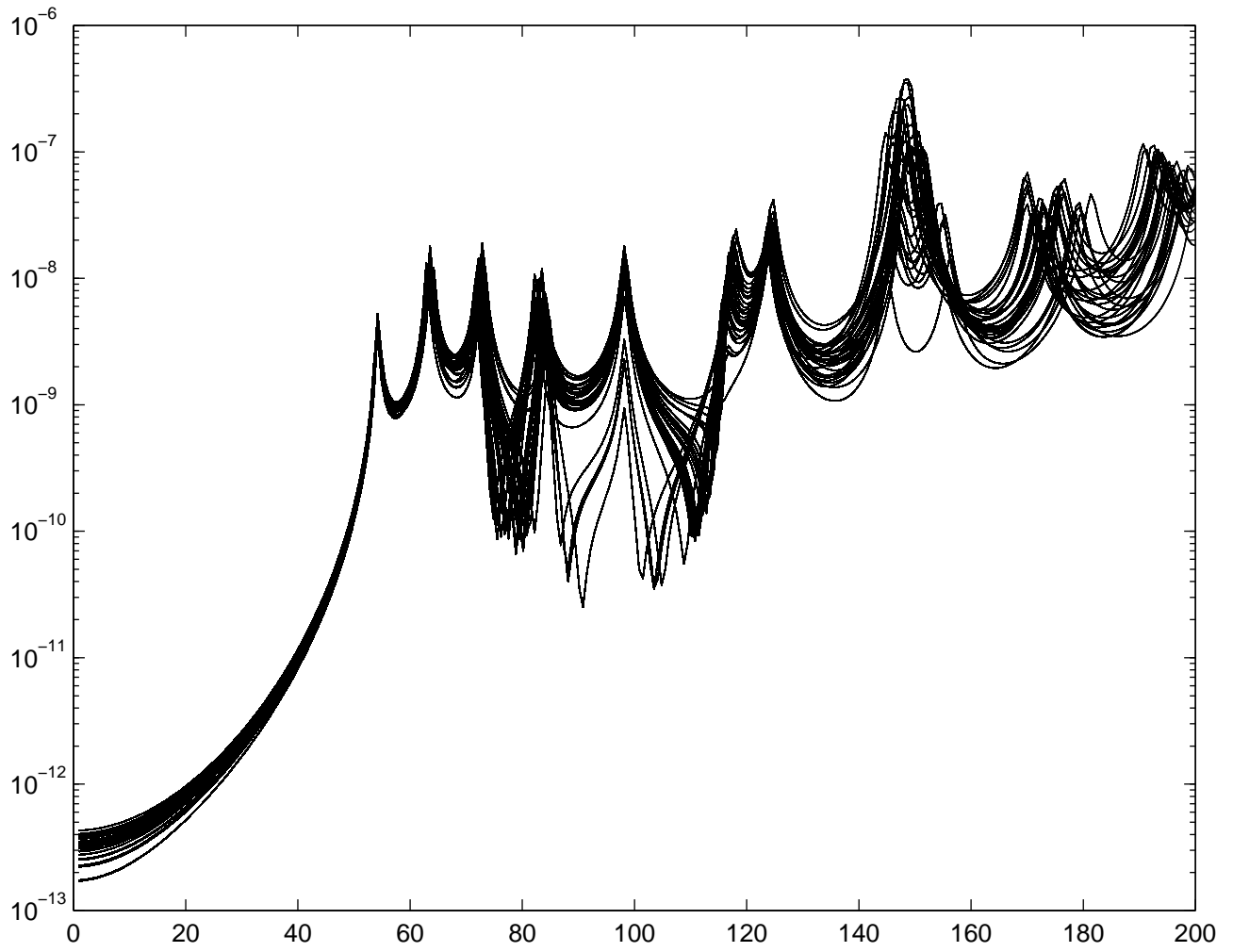


Figure 3: Displacement responses vs. frequency for variation of all connecting angles, 20 cases

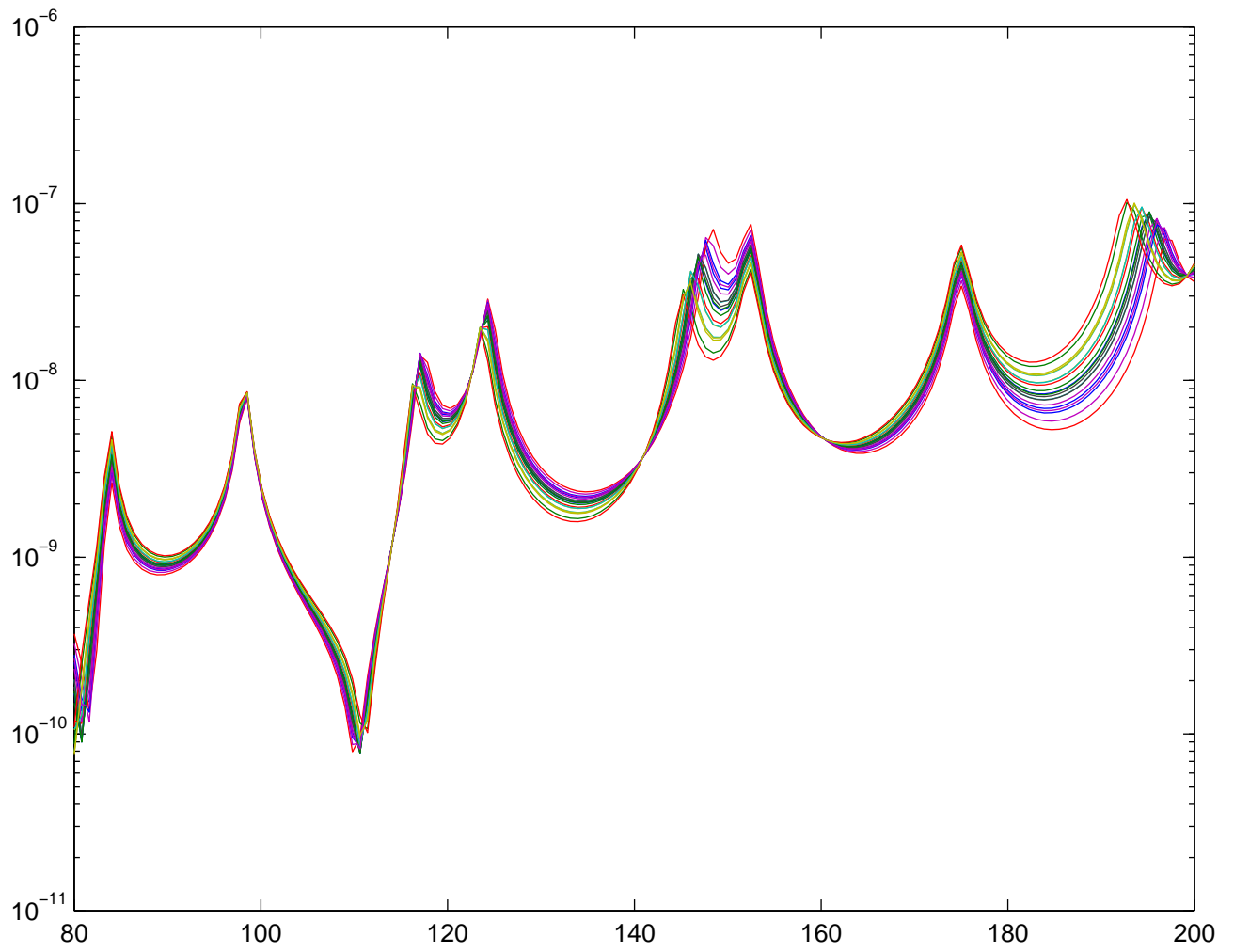


Figure 4: Sensitivity of connecting angle no 4. Displacement (m) versus Frequency (Hz). 20 cases

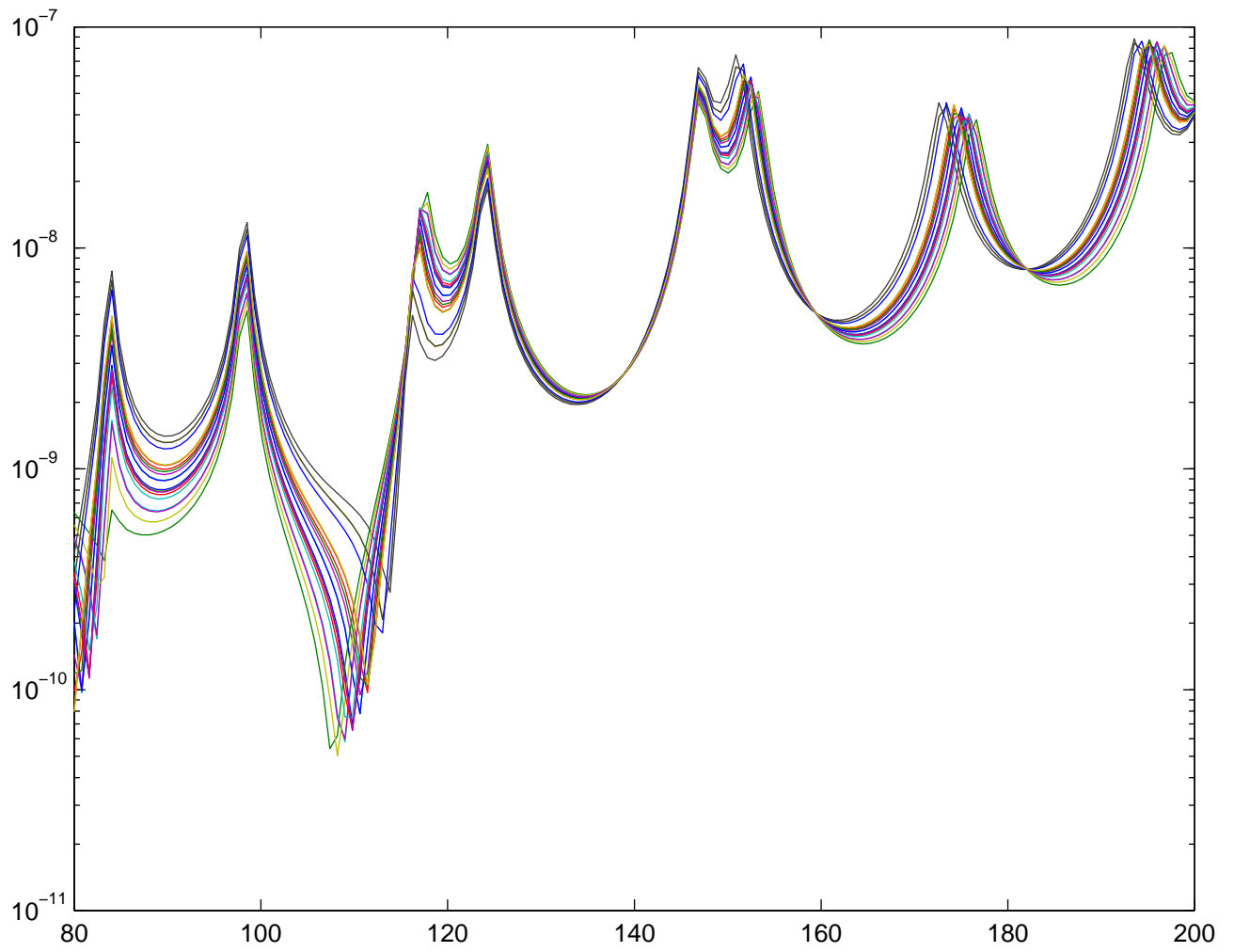


Figure 5: Sensitivity of connecting angle no 5. Displacement (m) versus Frequency (Hz). 20 cases

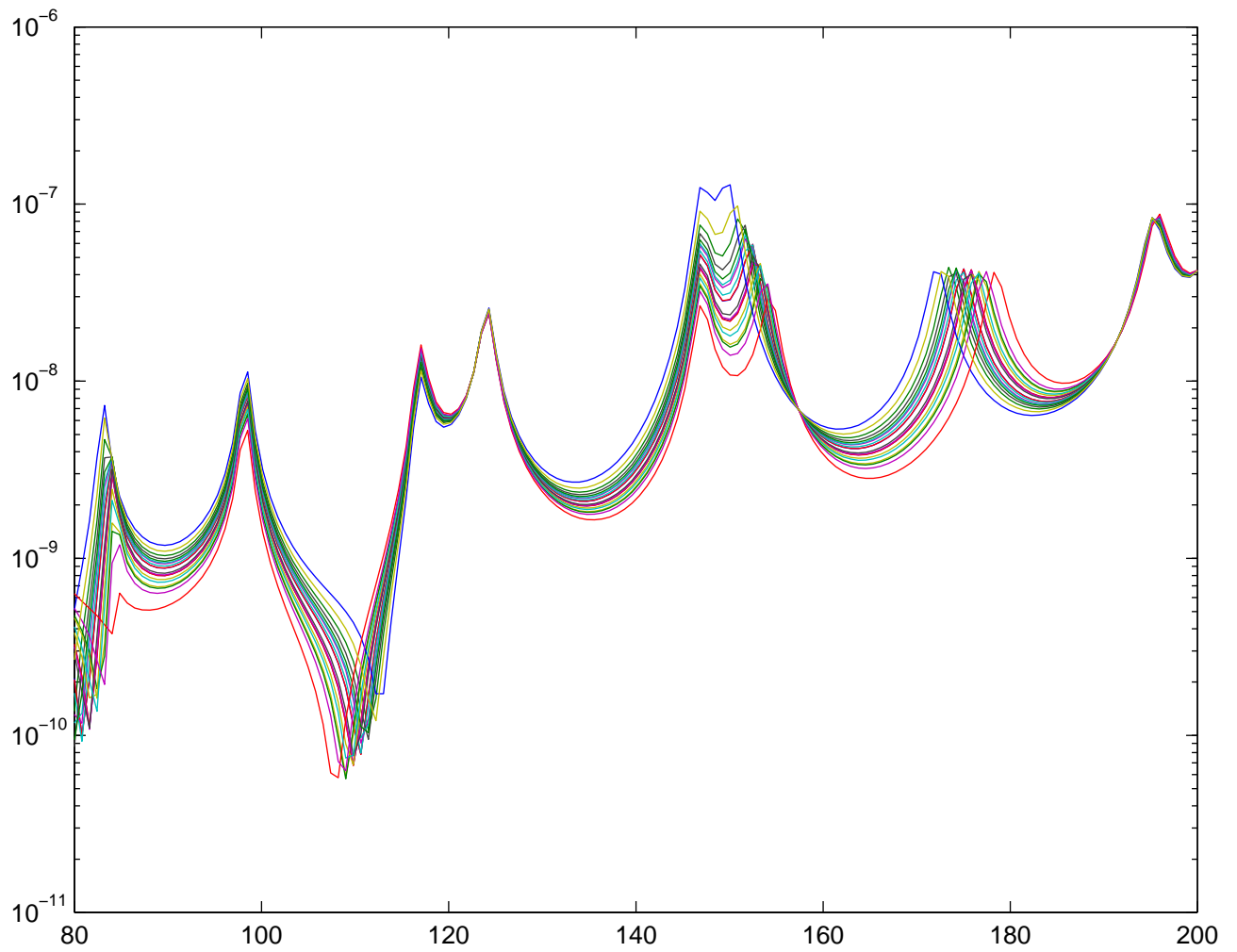


Figure 6: Sensitivity of connecting angle no 7. Displacement (m) versus Frequency (Hz). 20 cases

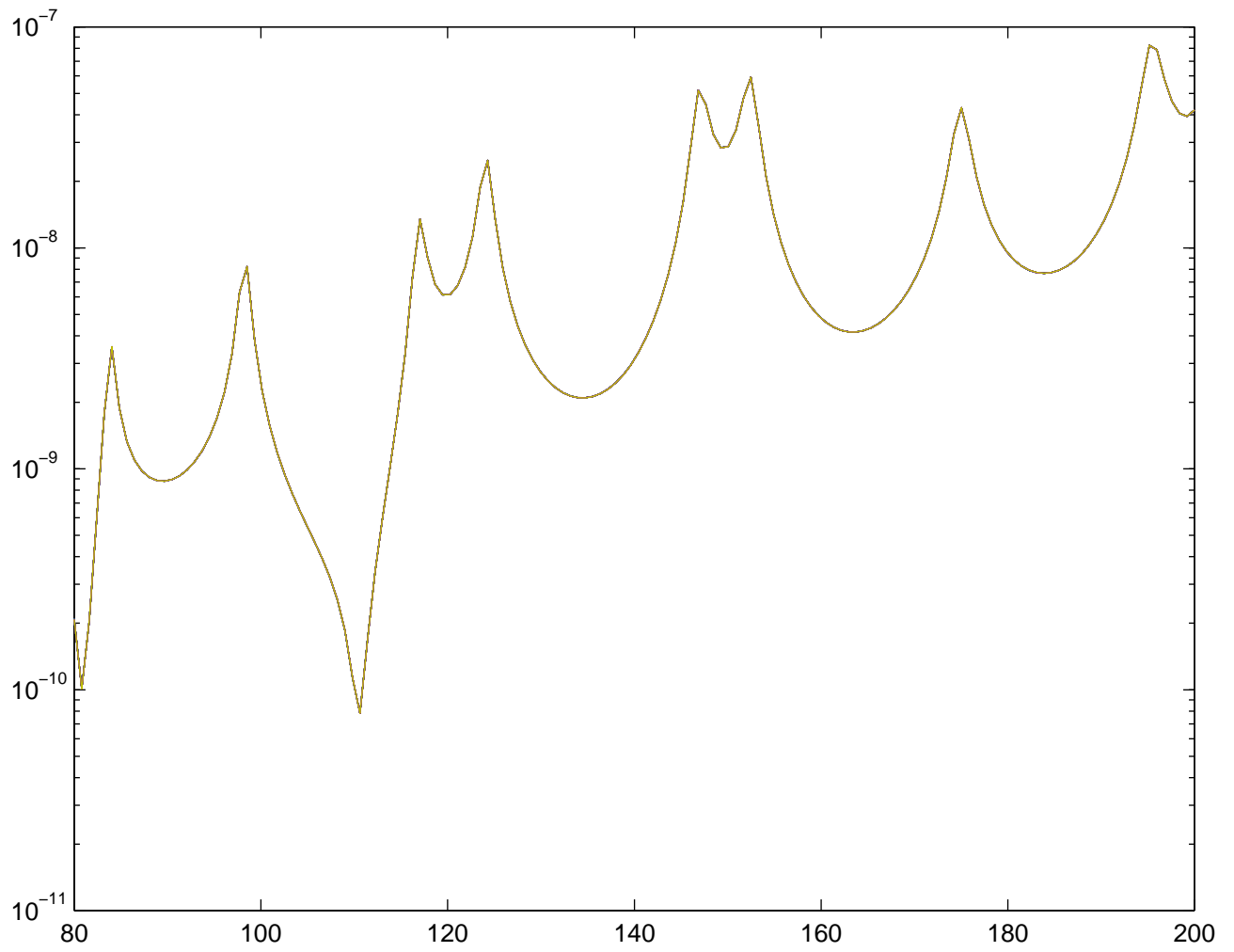


Figure 7: Sensitivity of other angles. Displacement (m) versus Frequency (Hz).
20 cases

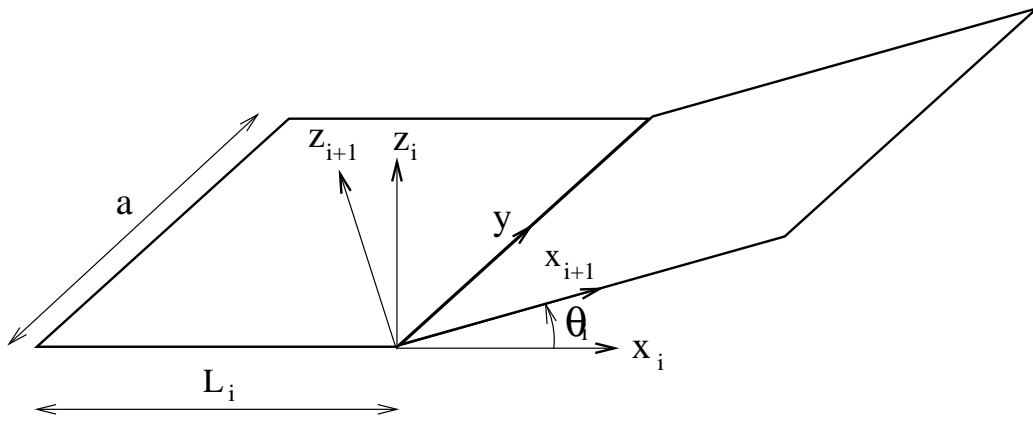


Figure 8: Notations for two coupled plates

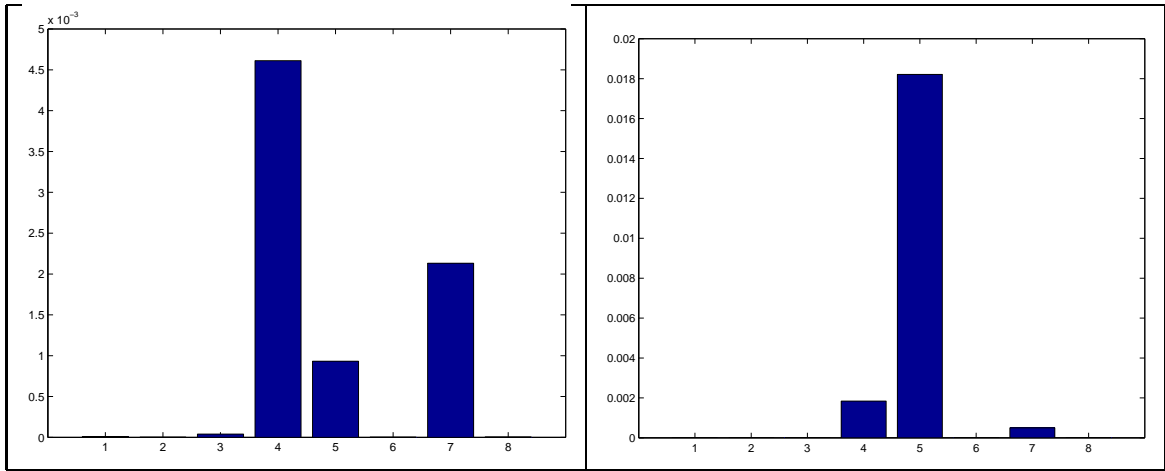


Figure 9: Residual value vs. connecting angle number, mean of 40 calculations, a) f=175 and b) f=195 Hz

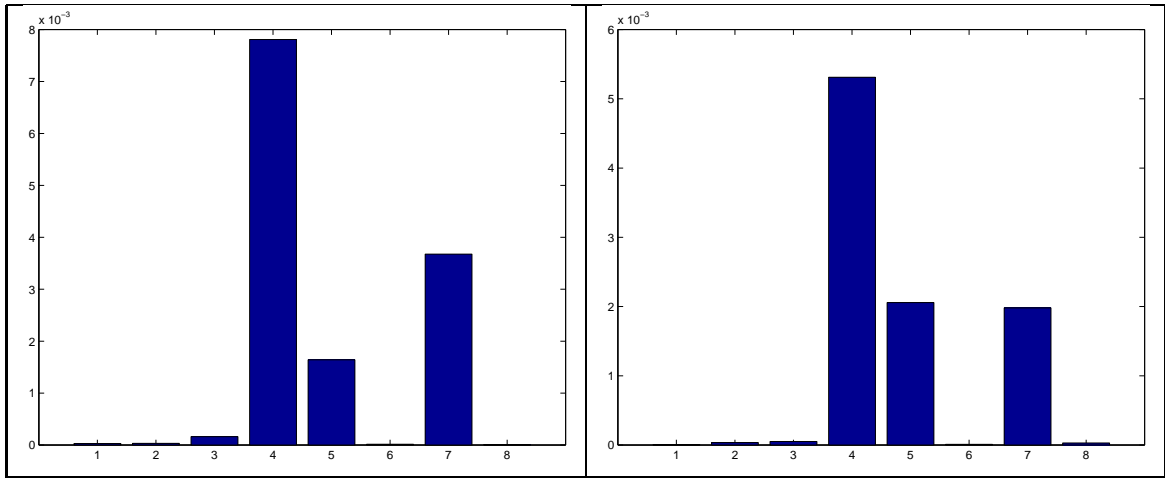


Figure 10: Residual value vs. connecting angle number, mean of 3 cases, $f=195$ Hz, a) 1st calculation b) 2nd calculation

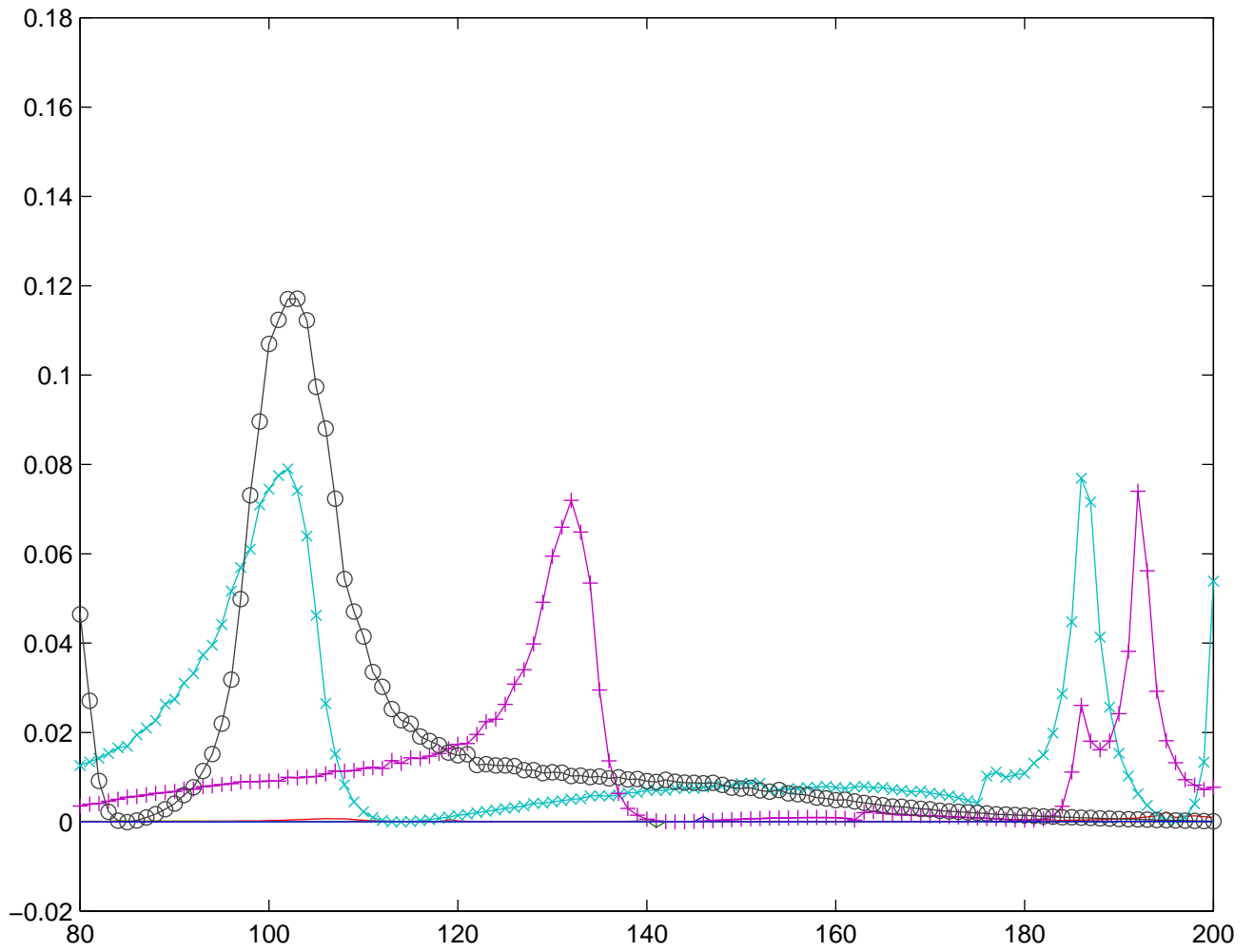


Figure 11: Residual value vs. frequency. Monte Carlo simulation 2000 cases -x- angle 4; +- angle 5; -o- angle 7; — other angles

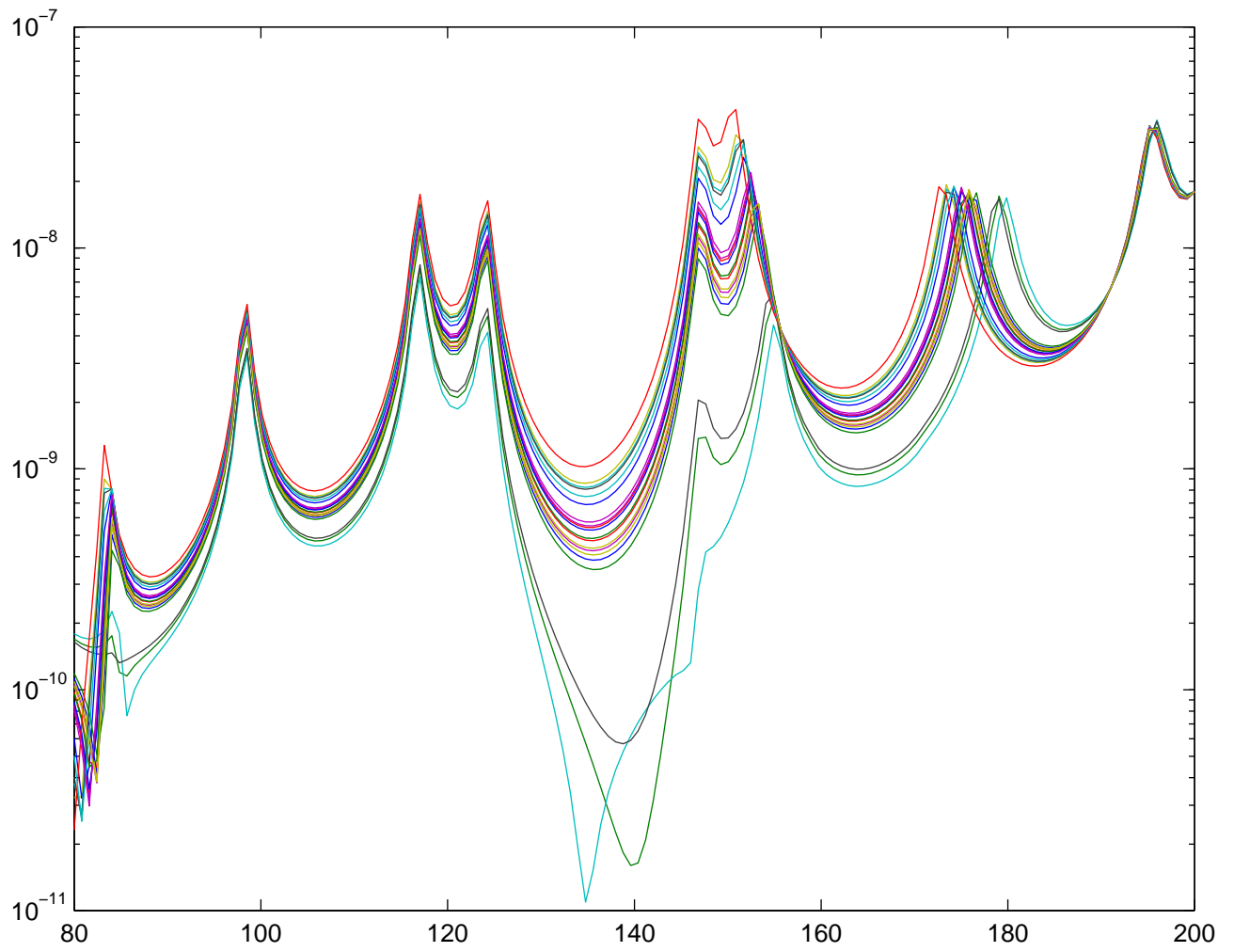


Figure 12: Sensitivity of connecting angle no 7. Displacement (m) versus Frequency (Hz). 20 cases

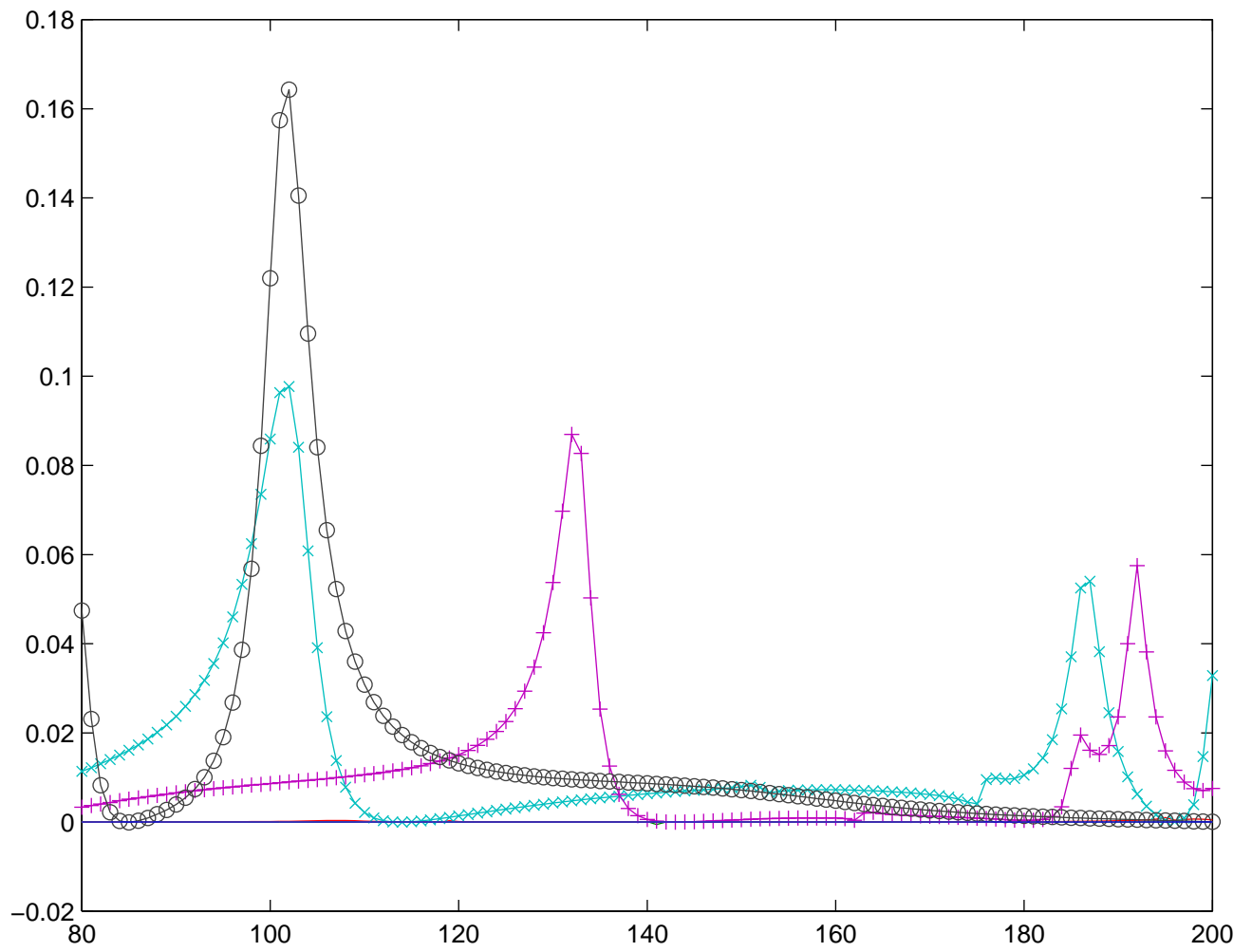


Figure 13: Evolution of first order linearisation of residual value vs. frequency

List of Figures

1	Rod model	22
2	Steel plates hypersensitive structure	23
3	Displacement responses vs. frequency for variation of all connecting angles, 20 cases	25
4	Sensitivity of connecting angle no 4. Displacement (m) versus Frequency (Hz). 20 cases	26
5	Sensitivity of connecting angle no 5. Displacement (m) versus Frequency (Hz). 20 cases	27
6	Sensitivity of connecting angle no 7. Displacement (m) versus Frequency (Hz). 20 cases	28
7	Sensitivity of other angles. Displacement (m) versus Frequency (Hz). 20 cases	29
8	Notations for two coupled plates	30
9	Residual value vs. connecting angle number, mean of 40 calculations, a) f=175 and b) f=195 Hz	31
10	Residual value vs. connecting angle number, mean of 3 cases, f=195 Hz, a) 1st calculation b) 2nd calculation	32
11	Residual value vs. frequency. Monte Carlo simulation 2000 cases -x- angle 4; +- angle 5; -o- angle 7; — other angles	33
12	Sensitivity of connecting angle no 7. Displacement (m) versus Frequency (Hz). 20 cases	34
13	Evolution of first order linearisation of residual value vs. frequency	35